JPNT 9(3), 207-214 (2020)
https://doi.org/10.11003/JPNT.2020.9.3.207

JPNT Journal of Positioning, Navigation, and Timing

Frequency Tracking Error Analysis of LQG Based Vector Tracking Loop for Robust Signal Tracking

Minhuck Park, Changdon Kee†

Department of Aerospace Engineering and the Institute of Advanced Machines and Design, Seoul National University, Seoul 08826, Korea

ABSTRACT

In this paper, we implement linear-quadratic-Gaussian based vector tracking loop (LQG-VTL) instead of conventional extended Kalman filter based vector tracking loop (EKF-VTL). The LQG-VTL can improve the performance compared to the EKF-VTL by generating optimal control input at a specific performance index. Performance analysis is conducted through two factors, frequency thermal noise and frequency dynamic stress error, which determine total frequency tracking error. We derive the thermal noise and the dynamic stress error formula in the LQG-VTL. From frequency tracking error analysis, we can determine control gain matrix in the LQG controller and show that the frequency tracking error of the LQG-VTL is lower than that of the EKF-VTL in all C/N0 ranges. The simulation results show that the LQG-VTL improves performance by 30% in Doppler tracking, so the LQG-VTL can extend pre-integration time longer and track weaker signals than the EKF-VTL. Therefore, the LQG-VTL algorithm is more robust than the EKF-VTL in weak signal environments.

Keywords: vector tracking loop, LQG, frequency tracking error, thermal noise, dynamic stress error

1. INTRODUCTION

Traditional GPS receivers use loop filter based scalar tracking loop (LF-STL). The receivers with the LF-STL track measurements of each channel independently and gather the measurements to calculate the user's position. Therefore, if an arbitrary channel is instantaneously disconnected, a signal lock loss occurs. In contrast, vector tracking loop (VTL) collects the discriminator outputs for each channel and estimates the user's position first. Then, the numerically controlled oscillator (NCO) input for each channel is calculated using the estimated position. In other words, even if one of the channel is momentarily disconnected, tracking lock can be maintained continuously using the estimated user's position.

Conventional VTL algorithm consists of a combination of the loop filter and extend Kalman filter (EKF) (So 2009). In this structure, the EKF estimates the user's position and the loop filter generates NCO input of each channel. The EKF is based on optimal estimation theory, but the loop filter is just filtering process dependent on order and bandwidth. To improve performance of tracking algorithm, linear-quadratic regulator (LQR) controller can be used instead of the loop filter. The combination of the EKF and the LQR controller is LQG controller, which is satisfied with not only optimal estimation theory but optimal control theory. The LQR controller estimates NCO inputs and guarantee optimal NCO input given performance index. How to design plant such as state transition matrix and control input is the most important factor in the LQR controller. We follow the reference's plant design (Kim et al. 2019).

In this paper, theoretical performance analysis of the LQG based VTL (LQG-VTL) is conducted compared to

Received May 14, 2020 **Revised** Jul 08, 2020 **Accepted** Jul 27, 2020
†**Corresponding Author**
E-mail: kee@snu.ac.kr
Tel: +82-2-880-1912 Fax: +82-2-878-8918
Minhuck Park https://orcid.org/0000-0001-5016-0115
Changdon Kee https://orcid.org/0000-0002-8691-7068

the EKF-VTL. Performance analysis is performed in terms of frequency tracking error. The frequency tracking error consists of thermal noise corresponding to the noise term and dynamic stress error corresponding to the bias term. The thermal noise and dynamic stress error equations of the LQG-VTL are derived and compare the performance according to control gain matrix tuning. The control gain matrix is determined by total frequency tracking error and the final tuned the LQG-VTL is compared with the EKF-VTL. We also define a tracking threshold and compare the trackable minimum C/N0 values of the EKF-VTL and the LQG-VTL.

This paper is organized as follows. In Section 2, we propose the LQG-VTL plant modeling. In Section 3, we derive theoretical frequency tracking errors of the LQG-VTL and define total frequency tracking error and tracking threshold. Using these terms, we perform how to find the best control gain matrix and compare the performance with the EKF-VTL. In Section 4, simulation results support above theoretical analysis results. Section 5 concludes the paper.

2. LQG–VTL STRUCTURE

The LQG based signal tracking loop are based on the plant modeling of the reference (Kim et al. 2019). In this plant modeling, the carrier-aided code tracking method is used for the code delay estimation, and the LQR controller estimates the variation of the code/carrier NCO inputs to control the term corresponding the acceleration variation. The states of the LQG based scalar tracking loop (STL) are the error values of all channels. An upper-case 'm' means number of visible satellites. The variable T is the pre-integration time (PIT).

$$\begin{pmatrix} \delta\tau_{k+1}^{1} \\ \vdots \\ \delta\tau_{k+1}^{m} \\ \delta\phi_{k+1}^{1} \\ \vdots \\ \delta\phi_{k+1}^{m} \\ \delta\dot{\phi}_{k+1}^{1} \\ \vdots \\ \delta\dot{\phi}_{k+1}^{m} \end{pmatrix} = \begin{bmatrix} 1 & & & T & & & \\ & \ddots & & & \ddots & & \\ & & 1 & & & T & \\ & & & 1 & T & & \\ & & & & \ddots & \ddots & \\ & & & & 1 & T & \\ & & & & & 1 & \\ & & & & & & \ddots \\ & & & & & & & 1 \end{bmatrix} \begin{pmatrix} \delta\tau_{k}^{1} \\ \vdots \\ \delta\tau_{k}^{m} \\ \delta\phi_{k}^{1} \\ \vdots \\ \delta\phi_{k}^{m} \\ \delta\dot{\phi}_{k}^{1} \\ \vdots \\ \delta\dot{\phi}_{k}^{m} \end{pmatrix} + \begin{bmatrix} T & & & & & & \\ & \ddots & & & & & \\ & & T & & & & \\ & & & 1 & & & \\ & & & & \ddots & & \\ & & & & & 1 & \\ & & & & & & 1 \end{bmatrix} \begin{pmatrix} \delta\Delta\hat{\tau}_{NCO,k}^{1} \\ \vdots \\ \delta\Delta\hat{\tau}_{NCO,k}^{m} \\ \delta\Delta\hat{\phi}_{NCO,k}^{1} \\ \vdots \\ \delta\Delta\hat{\phi}_{NCO,k}^{m} \end{pmatrix} + w_s \quad (1)$$

$$\rightarrow \delta x_{S,k+1} = F_S \delta x_{S,k} + G_S \delta u_k + w_{S,k}$$

$$\begin{pmatrix} \delta\tau_k^j = \text{j-th Code Tracking Error (m)} \\ \delta\phi_k^j = \text{j-th Carrier Phase Tracking Error (m)} \\ \delta\dot{\phi}_k^j = \text{j-th Carrier Freq. Tracking Error (m/s)} \end{pmatrix} \begin{pmatrix} \delta\Delta\hat{\tau}_{NCO,k}^j = \text{j-th } \delta\Delta CodeNCO \\ \delta\Delta\hat{\phi}_{NCO,k}^j = \text{j-th } \delta\Delta CarrierNCO \end{pmatrix}$$

To derive state equation of the LQG-VTL, the relationship between receiver tracking error and state of the VTL is as follows.

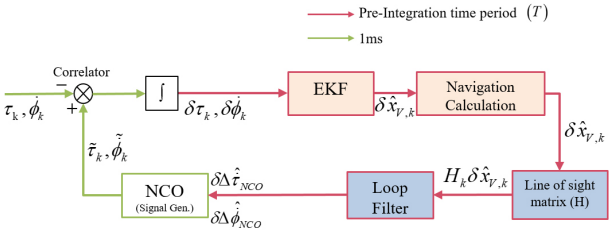

Fig. 1. EKF-VTL structure.

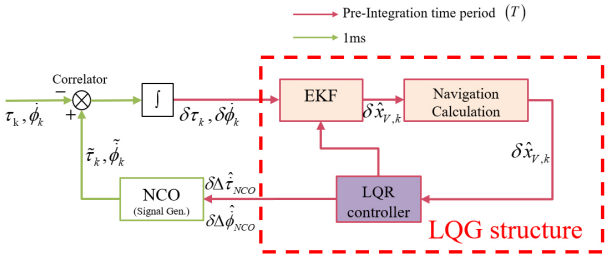

Fig. 2. LQG-VTL structure.

$$\begin{pmatrix} \delta\tau_k^1 \\ \vdots \\ \delta\tau_k^m \\ \delta\dot{\phi}_k^1 \\ \vdots \\ \delta\dot{\phi}_k^m \end{pmatrix} = -\begin{bmatrix} e_{x,k}^1 & e_{y,k}^1 & e_{z,k}^1 & & & & -1 & & \\ \vdots & \vdots & \vdots & & & & \vdots & & \\ e_{x,k}^m & e_{y,k}^m & e_{z,k}^m & & & & -1 & & \\ & & & e_{x,k}^1 & e_{y,k}^1 & e_{z,k}^1 & & -1 & \\ & & & \vdots & \vdots & \vdots & & \vdots & \\ & & & e_{x,k}^m & e_{y,k}^m & e_{z,k}^m & & -1 & \end{bmatrix} \begin{pmatrix} \delta p_{x,k} \\ \delta p_{y,k} \\ \delta p_{z,k} \\ \delta v_{x,k} \\ \delta v_{y,k} \\ \delta v_{z,k} \\ \delta B_k \\ \delta\dot{B}_k \end{pmatrix} \quad (2)$$

$$\rightarrow \delta x_{S,k} = H_k \delta x_{V,k}$$

$$\begin{bmatrix} e_{x,k}^j & e_{y,k}^j & e_{z,k}^j \end{bmatrix}^T : \text{j-th line of sight vector}$$

$$\begin{pmatrix} \begin{bmatrix} \delta p_{x,k} & \delta p_{y,k} & \delta p_{z,k} \end{bmatrix}^T : \text{position error (m)} \\ \begin{bmatrix} \delta v_{x,k} & \delta v_{y,k} & \delta v_{z,k} \end{bmatrix}^T : \text{velocity error (m/s)} \\ \delta B_k,\ \delta\dot{B}_k : \text{clock bias/drift error (m, m/s)} \end{pmatrix}$$

The above equation shows the relationship between the state of the STL and the VTL except for carrier phase measurement. This is because it is difficult to maintain vector phase-locked-loop (VPLL) without inertial navigation system (INS) or estimating atmospheric delay error. Therefore in this paper we use pseudorange and carrier frequency (Doppler) measurements as EKF measurements and we will take the VPLL into account in our future work. The measurement equation of the LQG-VTL can be derived by adding noise term in Eq. (2). Using line-of-sight matrix (H), the state equation in the LQG-VTL can be derived.

$$\begin{aligned} \delta x_{V,k+1} &= H_{k+1}^{\dagger} F_S H_k \delta x_{V,k} + H_{k+1} G_S \delta u_k + H_{k+1} w_{S,k} \\ \rightarrow \delta x_{V,k+1} &= F_V \delta x_{V,k} + G_V \delta u_k + w_{V,k} \end{aligned} \quad (3)$$

The states of the LQG-VTL are the error values of user position/velocity and clock bias/drift, and LQR controller inputs (δu_τ, δu_ϕ) are the variation of the code/carrier NCO inputs, same as the STL case. Figs. 1 and 2 show the block diagram of the EKF-VTL and the LQG-VTL respectively. In the EKF-VTL, NCO inputs are calculated by the loop filter. But in the LQG-VTL, the LQR controller, replacing the loop filter in the EKF-VTL, calculates NCO inputs and helps state propagation in Eq. (3). The relationship between the LQR control inputs and code/carrier NCO inputs are as follows. The matrix C is the LQR optimal gain matrix.

$$\begin{aligned}
&\delta u_k = \left[\delta u^1_{\tau,k} \quad \cdots \quad \delta u^m_{\tau,k} \quad \delta u^1_{\phi,k} \quad \cdots \quad \delta u^m_{\phi,k}\right]^T = -C\delta x_{V,k} \\
&CodeNCO^i_k = 1/\lambda_\tau \left(\dot{\phi}^i_k + \Delta CodeNCO^i_k\right) \\
&\qquad = 1/\lambda_\tau \left(\dot{\phi}^i_k + u^i_{\tau,k}\right) \qquad [chip] \qquad \left(\lambda_\tau = \frac{c}{f_{CA}}, \quad \lambda_f = \frac{c}{f_{L1}}\right) \\
&CarrierNCO^i_k = 1/\lambda_f \left(\dot{\phi}^i_k + \Delta CarrierNCO^i_k\right) \\
&\qquad = 1/\lambda_f \left(\dot{\phi}^i_k + u^i_{\phi,k}\right) \qquad [Hz]
\end{aligned} \tag{4}$$

The above equation shows the relationship between the state of the STL and the VTL except for carrier phase measurement. This is because it is difficult to maintain VPLL without inertial navigation system (INS) or estimating atmospheric delay error. Therefore in this paper we use pseudorange and carrier frequency (Doppler) measurements as EKF measurements and we will take the VPLL into account in our future work. The measurement equation of the LQG-VTL can be derived by adding noise term in Eq. (2). Using line-of-sight matrix (H), the state equation in the LQG-VTL can be derived.

Code and carrier tracking are also conducted by the LQR control input as shown in Eq. (4). The state space representation form is as follows. The estimated GPS measurements of all channels are denoted as z.

$$\begin{pmatrix} \tau^1_{k+1} \\ \vdots \\ \tau^m_{k+1} \\ \phi^1_{k+1} \\ \vdots \\ \phi^m_{k+1} \\ \dot{\phi}^1_{k+1} \\ \vdots \\ \dot{\phi}^m_{k+1} \end{pmatrix} = \begin{bmatrix} 1 & & & T & & & \\ & \ddots & & & \ddots & & \\ & & 1 & & & T & \\ & & & 1 & & & T \\ & & & & \ddots & & \ddots \\ & & & & & 1 & T \\ & & & & & & 1 \end{bmatrix} \begin{pmatrix} \tau^1_k \\ \vdots \\ \tau^m_k \\ \phi^1_k \\ \vdots \\ \phi^m_k \\ \dot{\phi}^1_k \\ \vdots \\ \dot{\phi}^m_k \end{pmatrix} + \begin{bmatrix} T & & & & \\ & \ddots & & & \\ & & T & & \\ & & & 1 & \\ & & & & \ddots \\ & & & & & 1 \end{bmatrix} \begin{pmatrix} \Delta\hat{\tau}^1_{NCO,k} \\ \vdots \\ \Delta\hat{\tau}^m_{NCO,k} \\ \Delta\hat{\phi}^1_{NCO,k} \\ \vdots \\ \Delta\hat{\phi}^m_{NCO,k} \end{pmatrix} \tag{5}$$

$$\rightarrow z_{k+1} = F_S z_k + G_S u_k$$

3. PERFORMANCE ANALYSIS LQG VECTOR TRACKING LOOP

3.1 Frequency Lock Loop Analysis

Table 1. Frequency thermal noise of LQG-VTL and EKF-VTL.

LQG-VTL	EKF-VTL (Lashley et al. 2009)
$\varepsilon = \phi_{rcv,k} - \phi_{pred,k} = \frac{1}{1+(G_{V,k}C_k)_{end}} C_k(x_{true,k} - \hat{x}^-_k)$	$\varepsilon = \phi_{rcv,k} - \phi_{pred,k} = H(x_{true,k} - \hat{x}^-_k)$
$\sigma^2_{tFLL} = E\left[\varepsilon\varepsilon^T\right] = \frac{1}{\left(1+(G_{V,k}C_k)_{end}\right)^2} C_k M_k C_k^T$	$\sigma^2_{tFLL} = E\left[\varepsilon\varepsilon^T\right] = HM_kH^T$

In this section, the performance analysis of the LQG-VTL is conducted using theoretical frequency tracking errors. The frequency tracking errors consist of thermal noise and dynamic stress error. The thermal noise which is the noise component of the error is typically expressed as a function of signal strength, filter design, and PIT. The dynamic stress error which is the bias component of the error is determined by user's dynamics and filter order. The thermal noise and the dynamic stress error in case of the EKF-VTL are derived from the reference (Lashley et al. 2009). In this paper, we modify the Lashley's method and apply the method to the LQG-VTL.

3.2 Frequency Thermal Noise of LQG-VTL

Frequency thermal noise of the LQG-VTL can be indirectly derived from the EKF prior covariance matrix. Measurement update and time update of the EKF are as follows.

$$\begin{aligned}
&\text{[Measurement update]} \\
&P_k = (I - K_kH_k)M_k(I - K_kH_k)^T + K_kR_kK_k^T \\
&\text{[Time update]} \\
&M_{k+1} = F_V P_k F_V^T + Q_k
\end{aligned} \tag{6}$$

When calculating NCO inputs, the EKF-VTL multiplies the line-of-sight matrix (H) by the deviation of user's position, but for LQG-VTL, control gain matrix (C) is used instead of H matrix. Also considering the control input in time update, the thermal noise (σ_{tFLL}) of the LQG-VTL can be derived. Table 1 shows frequency thermal noise of the LQG-VTL and the EKF-VTL.

3.3 Frequency Dynamic Stress Error of LQG-VTL

Frequency dynamic stress error occurs when the user's dynamics is higher than the filter order. For example, if a user performs a constant acceleration motion (3rd order) and the EKF state equation only estimates position and velocity (2nd order), the dynamic stress error will inevitably occur. In this paper, the dynamic stress error equation is derived assuming the above conditions.

The dynamic stress error of the LQG-VTL is also derived

from Lashley's idea. We consider two separate Kalman filters. One is the original Kalman filter which does not know the effects of the user's dynamics ($\hat{x}$). The second Kalman filter assumes that it knows the effects of the user's dynamics correctly ($\tilde{x}$). In this paper, we assume that user moves at constant acceleration (3rd order) and the EKF is comprised of position and velocity (2nd order). Also assume that up to k-th epoch, input acceleration (a) has been all zeros, which means that the states of the two EKF are identical until k-th epoch. In Lashley's method, the formula is derived in position domain and converted into range domain but in this paper we derive the formula directly in range domain.

User's acceleration motion can be reflected in the position domain as a matrix (B) and an input acceleration vector (a). In this case, we assume that acceleration occurs only in the x-direction.

$$\begin{aligned}&\tilde{x}_{V,k+1}^{-}=F_V\tilde{x}_{V,k}^{+}+B^d a\\&B^d=\begin{bmatrix}T^2/2 & 0 & 0 & T & 0 & 0 & 0 & 0\end{bmatrix}^T\end{aligned}\tag{7}$$

To convert the range domain, the line-of-sight matrix (H) is used. Also the differences between the two states prior to measurement update at (k+1)-th epoch are as follows.

$$\begin{aligned}&\tilde{z}_{k+1}^{-}=F_s\tilde{z}_k^{+}+HB^d a\\&\hat{z}_{k+1}^{-}=F_s z_k^{+}\\&\rightarrow \tilde{z}_{k+1}^{-}-\hat{z}_{k+1}^{-}=HB^d a=N_k^{-}a\end{aligned}\tag{8}$$

The differences between the two states after the measurement update are also derived as follows. Unlike in the EKF-VTL cases, the LQG-VTL should consider input vectors (u) in measurement update.

$$\begin{aligned}&\tilde{z}_{k+1}^{+}=\tilde{z}_{k+1}^{-}+G_s\tilde{u}_{k+1}\\&\hat{z}_{k+1}^{+}=z_{k+1}^{-}+G_s\hat{u}_{k+1}\\&\rightarrow \tilde{z}_{k+1}^{+}-\hat{z}_{k+1}^{+}=\left(\tilde{z}_{k+1}^{-}-z_{k+1}^{-}\right)-G_sC\left(\delta\tilde{x}_{k+1}-\delta\hat{x}_{k+1}\right)\\&\qquad=\left(I-G_sCK_{k+1}\right)\left(\tilde{z}_{k+1}^{-}-\hat{z}_{k+1}^{-}\right)\\&\qquad=\left(I-G_sCK_{k+1}\right)N_k^{-}a=N_k^{+}a\end{aligned}\tag{9}$$

Similarly, we can derive the formula at (k+2)-th epoch

$$\begin{aligned}&\tilde{z}_{k+2}^{-}=F_s\tilde{z}_{k+1}^{+}+HB^d a\\&\hat{z}_{k+2}^{-}=F_s z_{k+1}^{+}\\&\rightarrow \tilde{z}_{k+2}^{-}-\hat{z}_{k+2}^{-}=F_s\left(\tilde{z}_{k+1}^{-}-z_{k+1}^{-}\right)+HB^d a\\&\qquad=\left(F_sN_k^{+}+HB^d\right)a=N_{k+1}^{-}a\end{aligned}\tag{10}$$

Table 2. Frequency dynamic stress error of LQG-VTL and EKF-VTL.

LQG-VTL	EKF-VTL
Initialization	Initialization
$N_k^{-}=HB^d$	$N_k^{-}=HB^d$
Iteration until converge	Iteration until converge
$N_k^{+}=N_k^{-}-G_sCK_{k+1}N_k^{-}$	$N_k^{+}=N_k^{-}-HK_{k+1}N_k^{-}$
$N_{k+1}^{-}=HB^d+F_sN_k^{+}$	$N_{k+1}^{-}=HB^d+F_sN_k^{+}$
After converge	After converge
$\varepsilon=\dot{\phi}_{tcv,k}-\dot{\phi}_{pred,k}$	$\varepsilon=\dot{\phi}_{tcv,k}-\dot{\phi}_{pred,k}$
$f_e=E[\varepsilon_{ss}]=N_{ss}^{-}a$	$f_e=E[\varepsilon_{ss}]=N_{ss}^{-}a$

Table 3. Performance analysis environment.

Condition	Value
Dimension	2D
User's dynamics	Constant acceleration (7 m/s^2)
Measurements	Pseudorange (PR), Doppler (DP)
State	Position, Velocity
Number of satellites	3 (PDOP: 1.16, assume constant)
PIT	20 ms

The differences between two states mean the error caused by user's acceleration. Therefore, we can derive the frequency dynamic stress error (f_e) in the LQG-VTL using steady state value of matrix N. Table 2 shows iteration procedure to calculate frequency dynamic stress error of the LQG-VTL and EKF-VTL.

3.4 Total Frequency Tracking Error

Using thermal noise and dynamic stress error, we can define theoretical total frequency tracking error ($3\sigma_{FLL}$) as follows (Kaplan & Hegarty 2006).

$$3\sigma_{FLL}=3\sigma_{tFLL}+f_e\tag{11}$$

We can utilize the total frequency tracking error when tuning the control gain matrix in LQG-VTL. To determine the control gain matrix, we should tune state weighting matrix (A) and input weighting matrix (B). For example, we define the specific case briefly in Table 3. We conducted simulation in a simple 2D environment only for verifying tracking performance. In this 2D environment, three satellites are sufficient to calculate navigation solution. The values, x1 and x2, are the weighting factors of position and velocity respectively. The values, u1 and u2, are the weighting factors of the variation of the code and carrier NCO inputs respectively.

$$\begin{aligned}A&=\mathrm{diag}\left(\begin{bmatrix}1/x_1^2 & 1/x_1^2 & 1/x_2^2 & 1/x_2^2\end{bmatrix}\right)\\B&=\mathrm{diag}\left(\begin{bmatrix}1/u_1^2\cdots & 1/u_1^2 & 1/u_2^2\cdots & 1/u_2^2\end{bmatrix}\right)\end{aligned}\tag{12}$$

https://doi.org/10.11003/JPNT.2020.9.3.207

Table 4. Three tuning values.

	(x1, x2)	(u1, u2)
Tuning 1	(0.05, 1)	(2, 1)
Tuning 2	(0.5, 1)	(2, 1)
Tuning 3	(2, 1)	(2, 1)

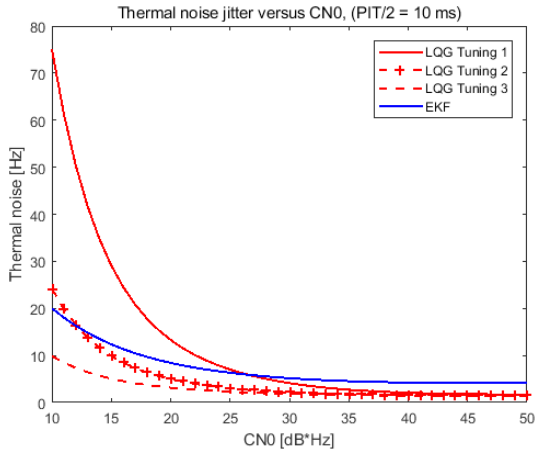

(a)

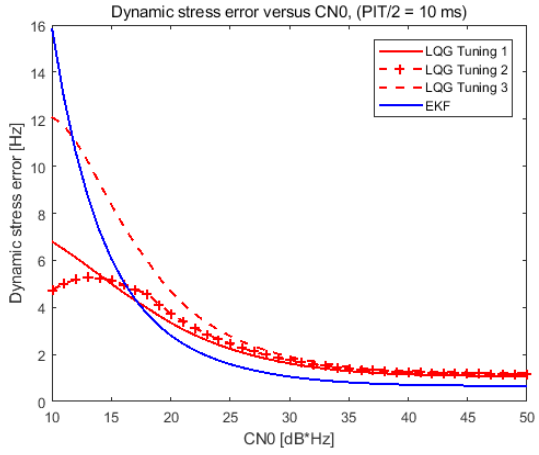

(b)

Fig. 3. Frequency tracking error. (a) thermal noise, (b) dynamic stress error

In a performance analysis environment, dilution of precision (DOP) and user's dynamics are the most important factors influencing the results. From the receiver designer's perspective, if you know the user's approximate maximum dynamics and DOP environment, you can find the theoretical dynamics stress error of LQG-VTL. To compare the effects of the tunings, the thermal noise, the dynamic stress error, and the total frequency tracking error are calculated for the three tunings. Table 4 shows three tuning values.

The theoretical thermal noise and dynamic stress error of LQG-VTL according to LQR tuning are as shown in Fig. 3. Also we draw the results of EKF-VTL under the same EKF

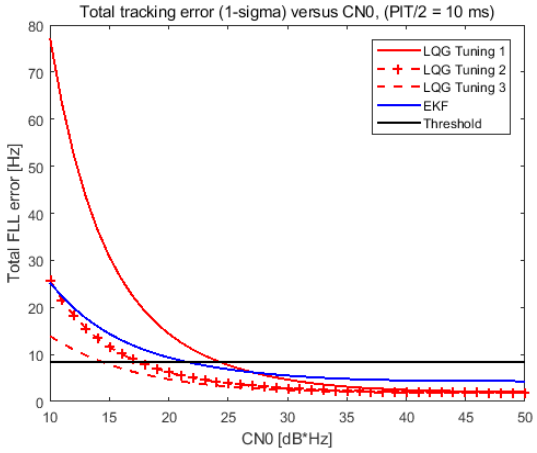

Fig. 4. Frequency total tracking error.

process noise and measurement noise tuning.

We can confirm that the thermal noise and the dynamic stress error are in various ranges depending on the tunings. Tuning 3, which is large dynamic stress error, is better in terms of thermal noise error. This trade-offs relationship between the thermal noise and the dynamic stress error makes it difficult to select proper control gain matrix tuning. To determine control gain matrix tuning, we calculate the total frequency tracking error as performance indicator. Fig. 4 shows the total tracking error of three tuning values.

In terms of total frequency tracking error, we can select tuning 3 as final tuning values. In this case, the thermal noise is weighted three times higher than the dynamic stress error, so tuning 3 with low thermal noise is selected as the final tuning value. If we adjust the weighing between thermal noise and dynamic stress error, other tuning values will be selected. This tuning values can be applied to any environment where the user's maximum dynamics is similar. Also tuning 3 shows lower error than EKF-VTL at all C/N0 ranges.

The theoretical total frequency tracking error also can be used as a tracking threshold analysis using following theory. The theoretical total frequency tracking error should not exceed the linear region of the FLL discriminator.

$$3\sigma_{FLL} = 3\sigma_{tFLL} + f_e \le \frac{1}{4T} \quad [Hz] \tag{13}$$

In this paper, we use sign(dot)(cross) discriminator and tracking threshold is defined as $1/(4T)$. This threshold can change depending on the type of the FLL discriminator. Fig. 5 shows the minimum C/N0 values not exceeding threshold according to PIT. We define this C/N0 values as trackable minimum C/N0. This values do not mean that signal tracking loop always loses signal lock below that

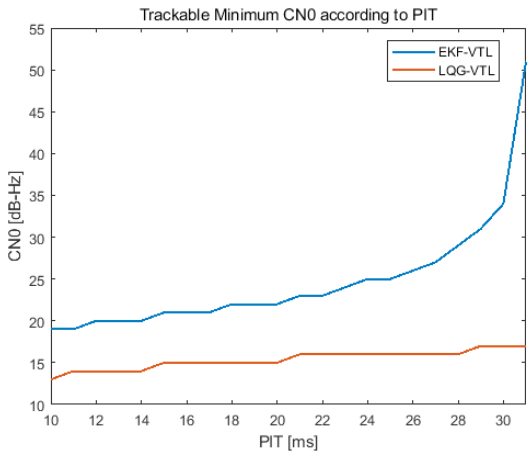

Fig. 5. Trackable minimum C/N0.

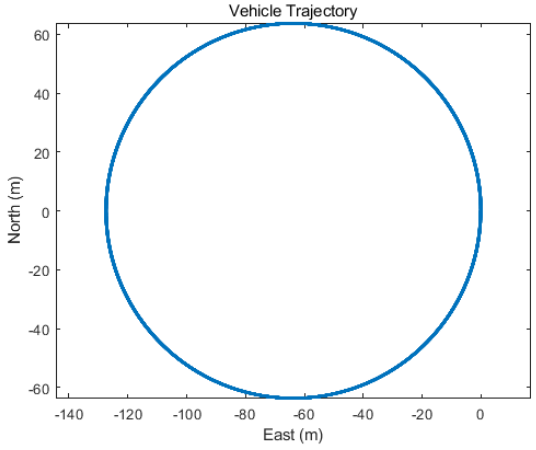

Fig. 6. User trajectory.

values. Instead, this values can be used as a guideline for the tracking threshold.

We can confirm that LQG-VTL can track at least 5 dB-Hz lower signal than EKF-VTL in all PIT ranges. This result shows LQG-VTL is more robust than EKF-VTL in high dynamics and low signal environments.

4. SIMULATION RESULTS

4.1 Simulation Tool & Setting

In Section IV, we demonstrate the ability of the LQG-VTL using developed simulation tool. The simulation tool is focused on signal tracking loop, and we can implement and verify the proposed tracking algorithm quickly before adapting software defined radio (SDR) receivers. The simulation tool consists of the following structures. First, set the input variables such as user/satellites motion, C/N0, and disturbance (atmosphere delay, multipath…). Second, generate reference GPS measurements: pseudorange, Doppler, and carrier phase. Third, calculate in-phase and quadrature measurements in correlator. Finally, test signal tracking algorithm such as the LQG-VTL and the EKF-VTL.

Table 5. Simulation setting.

Condition	Value
Dimension	2D
User's dynamics	Constant velocity circular motion (20 m/s, 1cycle / 20 sec)
Measurements	PR, DP
State	Position, Velocity
Number of satellites	3 (PDOP: 1.16, assume constant)

Table 6. Frequency RMS error (m/s).

PIT	1 ms	10 ms	20 ms	40 ms	50 ms	100 ms
EKF-VTL	1.68	1.54	1.54	X	X	X
LQG-VTL	1.12	1.06	1.05	1.06	1.08	X

Table 5 shows simulation setting. It is same as Table 3 except for user's dynamics. Since dynamic stress error derived in Section III assumes that the user dynamics is constant acceleration, it is not easy to apply directly in actual arbitrary user trajectory. In this case, maximum user acceleration is 6.3 m/s^2, which is similar to 7 used in the previous theoretical analysis (Table 3). Therefore, we can use same LQG tuning value, tuning 3. Fig. 6 shows user trajectory.

4.2 Performance Analysis According to C/N0 and PIT

Better frequency tracking performance enables the receiver to generate better replica signals, which means the receiver can track lower signal or extend PIT. Fig. 7 shows frequency root mean square (RMS) error according to C/N0 when 1 ms, 20 ms integration time respectively. The LQG-VTL improves performance 30% compared to the EKF-VTL in all C/N0 ranges. Especially when 20 ms PIT case, signal lock loss occurs less than 23 dB-Hz in the EKF-VTL case. While in the LQG-VTL case, the signal lock loss occurs less than 20 dB-Hz. Therefore the LQG-VTL can track 3 dB-Hz lower signal than the conventional EKF-VTL.

Table 6 shows frequency RMS error according to PIT at constant 40 dB-Hz signals. The EKF-VTL cannot extend PIT by more than 20 ms, but the LQG-VTL can extend PIT by up to 50 ms. This result shows the improved Doppler tracking performance can extend PIT in signal tracking loop.

Similar to the previous results, the LQG-VTL improve performance about 30% compared to EKF-VTL under 1, 10, 20 ms PIT conditions. The ability of the LQG-VTL to increase PIT longer also means it can track weaker signal.

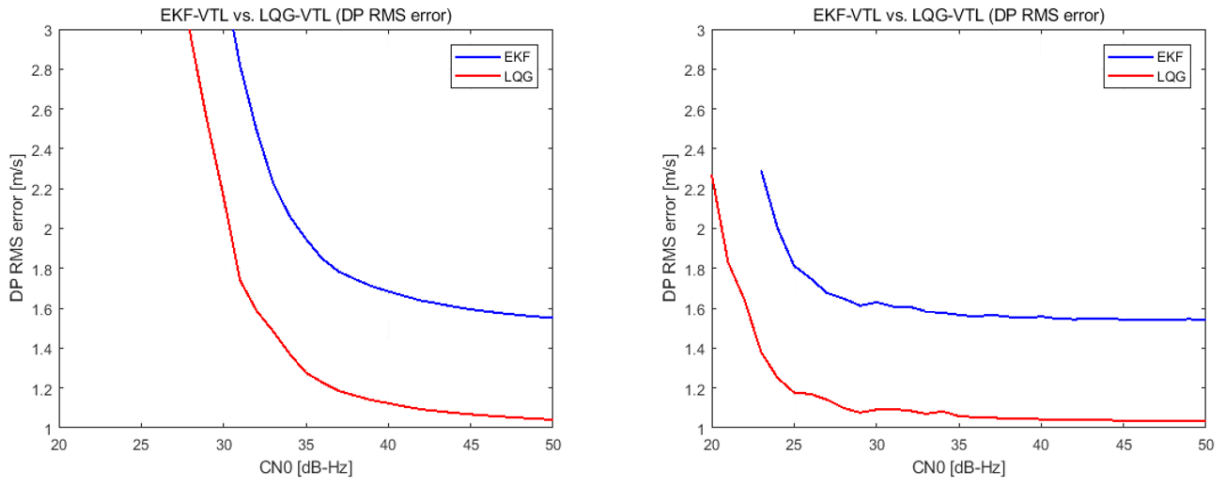

Fig. 7. Frequency RMS error. (a) PIT = 1 ms, (b) PIT = 20 ms

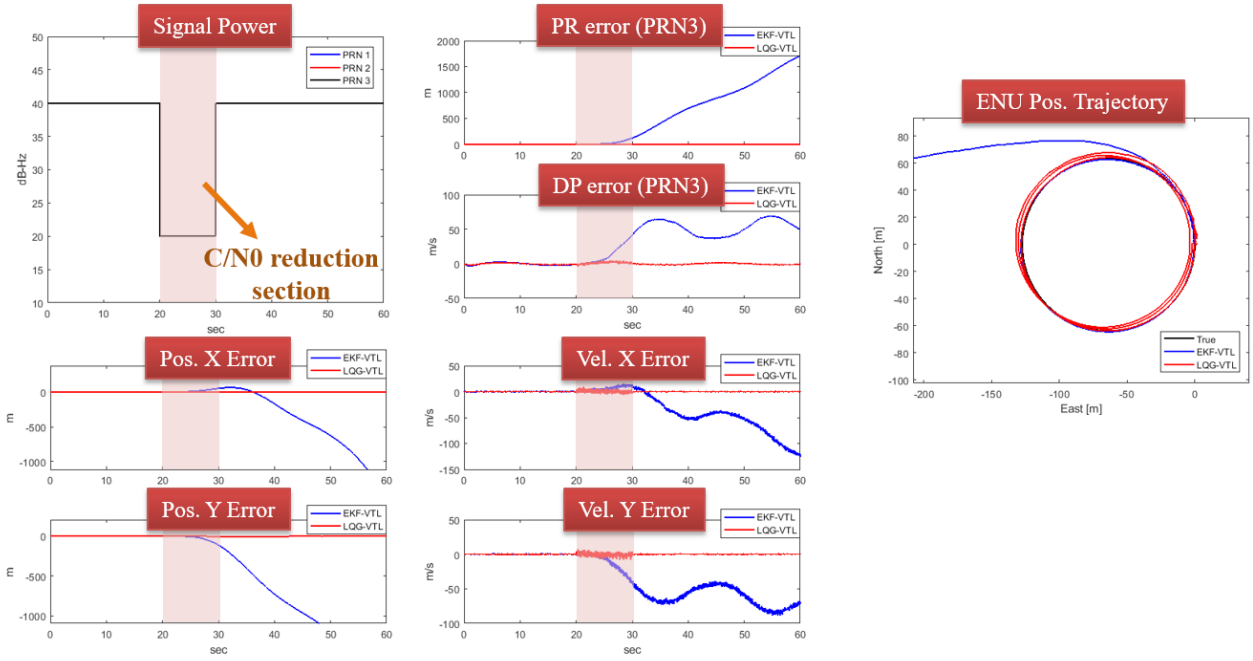

Fig. 8. Temporary signal power reduction case.

4.3 Temporary Signal Power Reduction Case

The last simulation is temporary signal power reduction case. A user rotates a period of 20 sec with a uniform circular motion of 20 m/s. Signal power of all channels decreases from 40 dB-Hz to 20 dB-Hz for 10 sec from 20 sec. The PIT of the receiver is 20 ms. We can expect the LQG-VTL can maintain the signal lock unlike the EKF-VTL as shown in Fig. 7. Fig. 8 shows all simulation results such as tracking errors and position/velocity errors. Only in the LQG-VTL case, pseudorange and Doppler tracking errors, and position/velocity errors converge under weak signal environments. The EKF-VTL cannot recover signal lock after the signal strength returns to 40 dB-Hz. In the East, North, Up (ENU) coordinates graph, the LQG-VTL can maintain circular shape continuously.

5. CONCLUSIONS

In this paper, we derive thermal noise and dynamic stress error of the LQG-VTL. Using these values, we can calculate

total frequency tracking error in the LQG-VTL. The total frequency tracking error can be used performance indicator to determine control gain matrix tuning. This tuning can be applied in any user with similar DOP and user's dynamics. When adapting best tuning values in the LQG-VTL, the total frequency tracking error of the LQG-VTL is lower than the EKF-VTL in all C/N0 ranges. Tracking threshold analysis confirms that the LQG-VTL can track at least 5 dB-Hz lower C/N0 signals than the EKF-VTL in all PIT ranges. Simulation results show the LQG-VTL can improve performance 30% in Doppler tracking error and extend PIT longer and track 3 dB-Hz lower signal than the EKF-VTL. Also the LQG-VTL can maintain the lock successively in temporary signal power reduction simulation.

ACKNOWLEDGMENTS

This research was supported by the "2019 CubeSat Contest" managed by the Korea Aerospace Research Institute (KARI) under the auspices of the Ministry of Science and ICT, contracted through by the Institute of Advanced Aerospace Technology at Seoul National University. We would like to thank KARI for their support. The Institute of Engineering Research at Seoul National University provided research facilities for this work.

AUTHOR CONTRIBUTIONS

Conceptualization, M.P. and C.K.; Methodology, M.P. and C.K.; Software, M.P.; Validation, M.P. and C.K.; Formal analysis, M.P. and C.K.; Investigation, M.P.; Writing-original draft preparation, M.P. and C.K.; Writing-review and editing, M.P. and C.K.; Supervision, C.K.; Project administration, C.K..

CONFLICTS OF INTEREST

The authors declare no conflict of interest.

REFERENCES

Kaplan, E. D. & Hegarty, C. J. 2006, Understanding GPS: Principles and Applications, 2nd ed. (Boston: Artech House)

Kim, C., Jeon, S., Park, M., Shin, B., & Kee, C. 2019, Optimal GNSS Signal Tracking Loop Design Based on Plant Modeling, International Journal of Aeronautical and Space Sciences, 20, 525-536. https://doi.org/10.1007/s42405-019-00141-0

Lashley, M., Bevly, D. M., & Hung, J. Y. 2009, Performance Analysis of Vector Tracking Algorithms for Weak GPS Signals in High Dynamics, IEEE Journal of Selected Topics in Signal Processing, 3, 661-673. https://doi.org/10.1109/JSTSP.2009.2023341

So, H. 2009, A Study on a Vector Tracking Loop Receiver for Pseudolite Navigation System, Ph. D. dissertation, Seoul National University, Seoul, Korea

Minhuck Park is a Ph.D. candidate of GNSS Lab. in the School of Mechanical and Aerospace Engineering at Seoul National University, South Korea. He received the B.S. and Master degree from Seoul National University. His research interests include GNSS Receivers, spoofing and GPS/INS integrated navigation system.

Changdon Kee is a Professor in the School of Mechanical and Aerospace Engineering at Seoul National University (SNU), South Korea and supervises SNU GNSS Lab (SNUGL, http://gnss.snu.ac.kr). He received B.S. and M.S. degrees from Seoul National University and a Ph.D. degree from Stanford University. He served as a Technical Advisor to the Federal Aviation Administration (FAA) on the Wide Area Augmentation System (WAAS) in 1994. Prof. Kee currently serves as a Technical Advisor for Korea Civil Aviation Safety Authority (KCASA) and Ministry of Public Administration and Security (MOPAS). He also served as a President of Korean Institute of Navigation. He has more than 20 years of GNSS and flight control research experiences.